RICE UNIVERSITY

Force Activation of a Multimeric Adhesive Protein through Domain Conformational Change

by

Sithara S. Wijeratne

A THESIS SUBMITTED
IN PARTIAL FULFILLMENT OF THE
REQUIREMENTS FOR THE DEGREE

Master of Science

APPROVED, THESIS COMMITTEE

Ching-Hwa Kiang, Chair
Associate Professor, Physics and Astronomy
Bioengineering

Yizhi Jane Tao, Associate Professor
Biochemistry and Cell Biology

Junichiro Kono, Professor
Electrical Engineering and Computer Science
Physics and Astronomy

HOUSTON, TEXAS
April 2012

ABSTRACT

Force Activation of a Multimeric Adhesive Protein through Domain Conformational Change

by

Sithara S. Wijeratne

The force-induced activation of adhesive proteins such as von Willebrand factor (VWF), which experience high hydrodynamic forces, is essential in initiating platelet adhesion. The importance of the mechanical force induced functional change is manifested in the multimeric VWF's crucial role in blood coagulation, when high fluid shear stress activates pVWF multimers to bind platelets. Here we showed that a pathological level of high shear flow exposure of pVWF multimers results in domain conformational changes, and the subsequent shifts in the unfolding force allow us to use force as a marker to track the dynamic states of multimeric VWF. We found that shear-activated pVWF multimers (spVWF) are more resistant to mechanical unfolding than non-sheared pVWF multimers, as indicated in the higher peak unfolding force. These results provide insight into the mechanism of shear-induced activation of pVWF multimers.

Acknowledgments

Foremost, I am thankful to my advisor, Professor Ching-Hwa Kiang, for her encouragement, patience, and support. Her guidance helped me to develop a better understanding of scientific research. I would also like to thank Professor Yizhi Jane Tao and Professor Junichiro Kono for serving on the thesis committee. Their comments and feedback to this work have been of great value.

I would like to express my gratitude to project collaborators, Dr. Jing-fei Dong of Baylor College of Medicine and University of Washington, and Dr. Joel M. Moake of Baylor College of Medicine and Rice University, for their expertise in designing this project. I also thank Hui-Chun Yeh, Zhou Zhou, Angela Bergeron and William May for preparing the protein samples.

In addition, I would like to thank my former and current group members for passing me their expertise. I am indebted to Eric Botello, who started the work reported here. I am grateful to Eric W. Frey for providing invaluable assistance and advice throughout this project. I also thank Jay M. Patel for his help.

Finally, I would like to express my deepest appreciation to my family and friends for their encouragement and support. I would like to thank my father, Tissa Wijeratne, and mother, Sumedha D. Wijeratne, and my sister, Rashmi S. Wijeratne, for their love and support throughout my life. I also sincerely thank Ardalan Amiri Sani for inspiring and motivating me to work hard through his strong work ethic. I dedicate this thesis to the memory of my late grandfather, R. M. Jayaweera.

Contents

List of Figures

Nomenclature

VWF	Von Willebrand Factor
pVWF	Plasma von Willebrand Factor
spVWF	Sheared plasma von Willebrand Factor
ULVWF	Ultra-large von Willebrand Factor
AFM	Atomic Force Microscope
WLC	Wormlike Chain

Chapter 1

Introduction

1.1. The Role of VWF in Blood Clotting

The mechanism of hemostasis arrests bleeding at the site of an injured blood vessel and initiates the tethering of platelets to von Willebrand factor (VWF) onto the subendothelium. The adhesion activity of plasma VWF (pVWF) multimers depends on two factors: multimer size and shear stress. Ultra-large (ULVWF) contains high avidity binding sites for platelets, and thus it spontaneously binds with platelet GPIBα once it is released. Exposure to high shear stress activates VWF (spVWF) and the capacity of pVWF multimers to bind to platelets increases. This activation VWF, which experience high hydrodynamic forces, is essential in maintaining hemostasis. Understanding the shear-induced activation mechanism of VWF is still under a subject of broad interest. The following sections will introduce the structure, biosynthesis and the mechanical activation of VWF.

1.2. Structure and Biosynthesis of VWF

Von Willebrand factor (VWF) is a large multimeric protein constructed from two identical VWF monomers linked by C-terminal disulfide bonds into dimers tail-to-tail at their CK regions, and the dimers then polymerize via head-to-head at the N-terminus of the D3 domain into long VWF multimers [1-5]. The domain organization of a 250 kDa, 60 nm long VWF monomer [3, 6] is shown in Fig. 1.1. Each monomer consists of 2050 amino acids separated into 12 different domains with two distinct regions, a globular and rod-like region; The domains in the mature VWF subunit are D'-D3-A1A2-A3-D4-B1-B2-B3-C1-C2-C3-CK.

Each individual domain in the VWF monomer contributes to the functionality of VWF. The tandem A domains each play a role in the VWF interaction, including cell adhesion. The structures of the A1 and A2 domain are shown in Fig. 1.2. The A1 domain consists of a compact α and β fold surrounded by a single disulfide loop, which binds to collagen and the platelet GPIbα [7, 8]. The structure of the A2 domain resembles the VWF fold with α-helices and β-strands that alternate in sequence, lacking an α4-helix [9]. The A2 contains the cleavage site of metalloprotease ADAMTS-13, a member of the "a disintegrin and metalloprotease with thrombospondin" repeats family of proteases [4, 10], which circulates in human plasma and is released constitutively from human ECs [10]. This cleavage mechanism inhibits the excessive adhesion and aggregation of platelets.

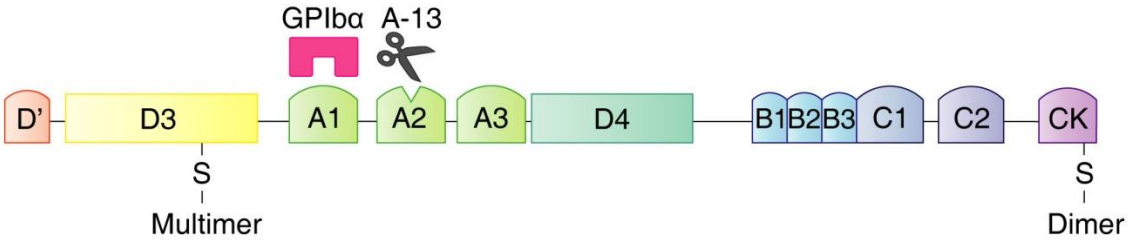

Fig. 1.1. The domain organization of a VWF monomeric subunit. A1 is the platelet glycoprotein Ib-IX-V receptor binding domain and A2 contains the cleavage site for ADAMTS-13. The monomers are linked through disulfide bonds in the C-terminal CK domains to form dimers, and the dimers are linked through the disulfide bonds in the N-terminal D3 domains to form *n* multimers.

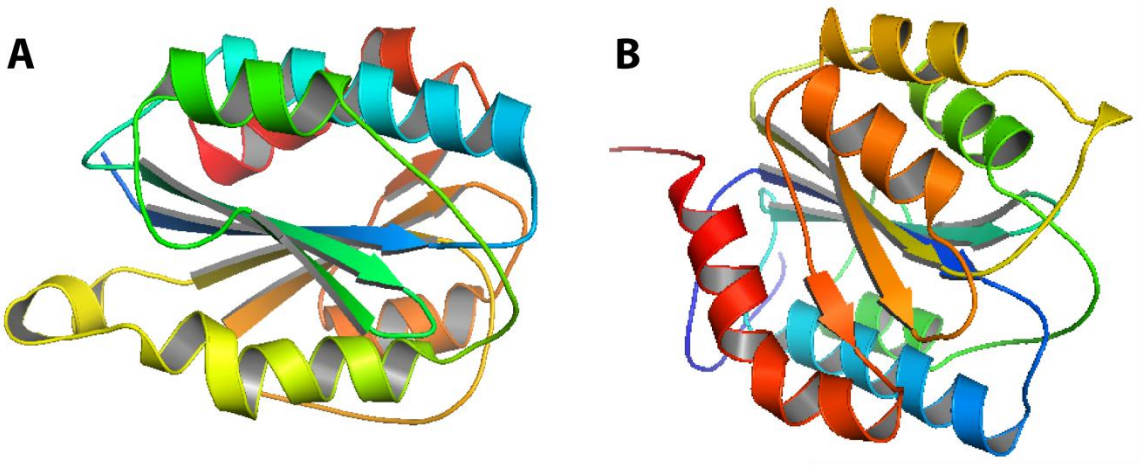

Fig. 1.2. Ribbon diagram of the (A) A1 domain and (B) A2 domain structure in the VWF monomer.

The largest VWF multimers contain up to 200 monomers [11] and are concentrated after synthesis in Weibel-Palade bodies and α-granules, the storage compartments of endothelial cells and platelets, respectively [3]. In response to stimulation by cytokines and other agents, these ultra-large VWF (ULVWF) multimers are rapidly secreted in long string-like structures by endothelial cells (ECs), to which they are anchored. EC-anchored ULVWF multimeric strings are hyper-adhesive in their capacity to bind platelet glycoprotein (GP) Ib-IX-V

complexes [5, 12]. EC-anchored ULVWF multimeric strings are cleaved by ADAMTS-13 [4, 10] into circulating plasma-type VWF (pVWF) multimers that vary over a wide range of molecular mass [4, 13]. The disease thrombotic thrombocytopenic purpura (TTP) is caused by mutations or inhibitions of ADAMTS-13 by antibodies causing an accumulation of ULVWF eventually resulting in platelet-rich microthrombi in the microvasculature [14]. The accumulation of ULVWF is considered to be responsible for the systemic thrombosis in microvasculature associated with thrombotic thrombocytopenic purpura. The loss of these large multimers results in a sub-type of von Willebrand disease.

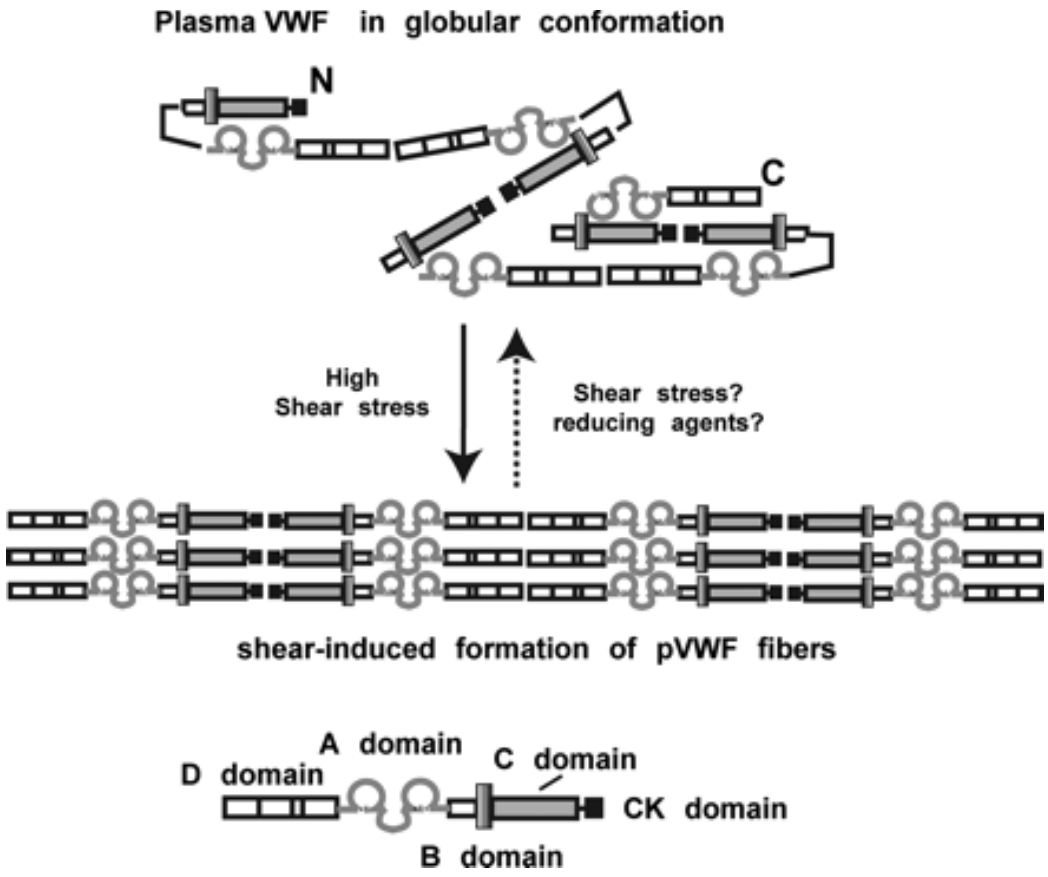

Fig. 1.3. Schematic illustration of covalent lateral association of a VWF multimer. From Ref. [4].

1.3. Shear-Induced Activation of pVWF

Circulating pVWF multimers are hemostatically inactive toward platelets, but can be activated by being exposed to high shear stress [3, 4, 15]. Fluid shear stress (in dynes/cm^2) in a tubular blood vessel is the force per unit area applied to blood flow [16]. It has been proposed that, under high shear stress, pVWF multimers undergo a change in conformation from a globular to an elongated form [3, 15, 17]. More recently, it has been demonstrated that shear-activated pVWF (spVWF) multimers become laterally apposed into fibrils via multimer-to-multimer disulfide bonds [18] (Fig. 1.3). The abundance of cysteine amino acids is also the root of VWF's conformational change that promotes VWF's adhesion to the subendothelial wall and nearby platelets. The lateral association aligns multiple VWF A1 domains to increase binding avidity and bond strength for platelet GPIbα. .

The shear-induced change in conformation exposes or alters the A1 domain in VWF monomeric subunits, enabling large VWF multimers to bind to platelet GP Ib-IX-V and initiate platelet adhesion or aggregation. The difference in the dynamic states of different forms of VWF multimers determines the on-off switching of VWF multimeric activation for platelet binding.

In this study, we used single-molecule manipulation to evaluate the force response of different forms of VWF multimers. The peak force was used as an indicator of the dynamic states of VWF monomeric subunit domains within VWF multimers. The following chapter will highlight the experimental procedures used in this research.

Chapter 2

Experimental Procedures

2.1. Materials and Methods

The following sections describe the materials and methods used in this work. The VWF sample preparation was performed by our collaborators at the Department of Medicine, Baylor College of Medicine and Department of Bioengineering, Rice University.

2.1.1. Purified pVWF multimers and soluble ULVWF multimers

pVWF was purified from the cryoprecipitate fraction of human plasma by glycine and NaCl precipitation and chromatography on a Sepharose 4B column. Endothelial cells were obtained from human umbilical veins (HUVECs). HUVECs were stimulated with100 μM histamine for 30 min, and VWF multimers enriched in soluble ULVWF multimers were collected.

2.1.2. Shear stress in the cone-plate viscometer

In order to generate spVWF, purified pVWF multimers (10 μg/ml) were exposed to 100 dyn/cm^2 of shear stress for 3 min at 37^{o}C on a cone-and-plate viscometer. The surface of the cone and plate was coated with 5% liquid silicone at room temperature overnight and rinsed gently before experiments. The shear stress applied was calculated based on a constant shear rate 10,000 s^{-1} and a viscosity of 1 cp for pVWF multimers in solution.

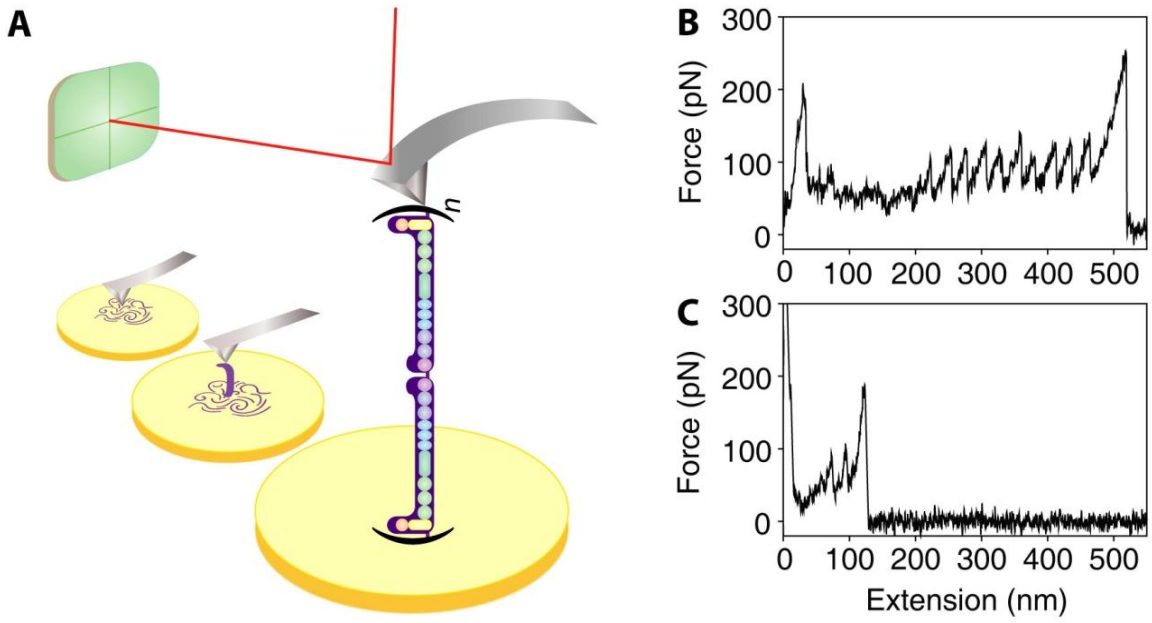

Fig. 2.1 Single-molecule pulling by AFM and force-extension curves. (A) Illustration of single-molecule pulling by AFM. A purified pVWF multimer, composed of polymerized dimers of VWF monomeric subunits, was adsorbed onto a gold substrate and brought into contact with an AFM tip. As the stage moved away from the tip, the VWF multimer was pulled while the force was recorded. Force-extension curve of (B) a pVWF multimer, and (C) a pVWF dimer. Each curve represents a single pVWF multimer molecule stretched at a constant velocity of 1000 nm/s.

2.2. Single-molecule AFM Experiments

Single-molecule manipulation is a powerful technique for probing the interactions and mechanical properties of individual proteins on a nanometer scale. These experiments will allow us to obtain information that is previously inaccessible with experiments.

2.2.1. Atomic Force Microscopy (AFM) Experiments

An atomic force microscope (AFM) was used to perform single-molecule manipulation of pVWF multimers, ULVWF multimers and spVWF multimers (see Fig. 2.1A). Multimeric VWF molecules were equilibrated at 37 °C prior to being deposited onto a fresh gold surface at room temperature for 10 minutes. The AFM tip was brought in contact with the surface for 1-3 seconds in order to establish a contact between the VWF multimeric molecule under study and the cantilever tip.

All of the force measurements were taken in aqueous buffer [phosphate-buffered saline (PBS), pH 7.4] with pulling velocities ranging from 100 nm/s to 5000 nm/s. For spVWF multimers, the pVWF multimers were exposed to shear stress as described above, and the time-dependent pulling experiments were performed starting at 30 minutes after shear exposure. Each experiment lasted from one to three hours. The time for each group is expressed as the mid-point of the time window of the data for that group. The time-dependence experiments were conducted on spVWF multimers at room temperature, and the force versus time data were converted to force versus molecular end-to-end distance curves (Fig.

2.1B, C). Histograms of force peaks were grouped and the distributions were fitted to a Gaussian curve. The peaks of these Gaussian curves represent the most probable unfolding forces.

2.3. Data Analysis

2.3.1. Wormlike chain (WLC) model

The force curve was fitted with a wormlike chain (WLC) model of polymer physics,

$$F(x) = \frac{k_B T}{L_p}\left(0.25(1-\frac{x}{L_c})^{-2} - 0.25 + \frac{x}{L_c} \right) \quad (1)$$

where L_p and L_c are the persistence length and the contour length, respectively, T is the temperature, and k_B is the Boltzmann constant. The equation is expressed as the force F as a function of distance x. This model utilizes two key parameters to describe the force extension curves: the persistence length, L_p, and the contour length, L_c. L_c specifies the length of the segment of the molecule being pulled (Fig. 2.1A), and L_p defines the stiffness of the molecule against bending.

2.3.2. Arrhenius Equation

The activation free energy barrier from spVWF to pVWF can be estimated from the rate reaction equation,

$$k = A\exp(-\Delta G / k_B T), \quad (2)$$

where $k = 1/\tau$ is the rate constant, ΔG is the free energy of barrier from spVWF to pVWF, k_B is the Boltzmann constant, T is temperature, and A is the pre-exponential factor. We assumed that A is between $10^5 s^{-1}$ and $10^7 s^{-1}$.

2.3.3. Time Relaxation Equation

From the first order reaction, the rate law from sheared to an unsheared state is

$$-\frac{d[S]}{dt} = k[S], \quad (3)$$

where S is the sheared state, and k is the first order rate constant. We can integrate Eq. 3 to yield the exponential decay equation $[S] = C_0 e^{-k_B T}$. The weighted average of the force is $F(t) = F_s \cdot S + F_P \cdot P$, where F_s is the force of spVWF, F_P is the force of pVWF and S and P are the fraction of sheared shear and unsheared molecules, respectively. From the conservation of mass, the relation, $P(t) + S(t) = 1$. Thus, solving for $P(t)$ and plugging the exponential decay equation to $F(t)$ yields,

$$F(t) = F_P - (F_P - F_s)e^{-t/\tau}. \quad (4)$$

Chapter 3

Results and Discussion

3.1. Speed-Dependence of VWF Multimers

We used an atomic force microscope (AFM) to pull single VWF multimeric molecules while measuring the force, as determined by the bending of the cantilever (Fig. 2.1A). The saw tooth patterns of force peaks in the force-extension curves of VWF multimers (Fig. 2.1B, C) are characteristic of multi-domain protein unfolding [19-21]. The value of the peaks specifies the force required to unfold the domains, and is related linearly to the unfolding free energy barrier and logarithmically to the pulling speed [20, 22, 23]. The force curves were fitted with a wormlike chain (WLC) model of polymer physics; see Eq. 1 in Chapter 2 [24-26]. The most probable unfolding forces as a function of pulling velocity (Fig. 3.1) were plotted. ULVWF multimers contain a larger number of monomers than pVWF, and are more active in adhering to platelets and inducing platelet aggregation [27]. We observed

differences in peak unfolding forces at high pulling speeds between ULVWF and pVWF multimers (Fig. 3.2), indicating that pVWF multimers and ULVWF are in different conformational states.

At high levels of shear stress (60-120 dyn/cm^2), the capacity of pVWF multimers to adhere to, and aggregate to platelets increases [27]. That is, sheared pVWF multimers become functionally similar to ULVWF multimers. The peak unfolding force of pVWF multimers increased after exposure to high shear stress, but the force-extension curves are qualitatively similar to unsheared pVWF multimers and unsheared ULVWF multimers. The difference in the peak unfolding forces between pVWF multimers and either spVWF or ULVWF multimers was more pronounced at high pulling velocities (Fig. 3.2). This finding is compatible with the shear-induced conformational change in pVWF (to spVWF) that increases the exposure of platelet-binding A1 domains in the VWF monomeric subunits of spVWF multimers. It has been shown that exposure to a 100 dyn/cm^2, high fluid shear stress induces pVWF multimers to associate laterally and form VWF fibrils (the conformational state of spVWF) that have an increased capacity to bind to platelet GPIbα receptors [4]. This fibrillar state of laterally-associated VWF multimers may be the conformation of spVWF multimers that is functionally similar to ULVWF.

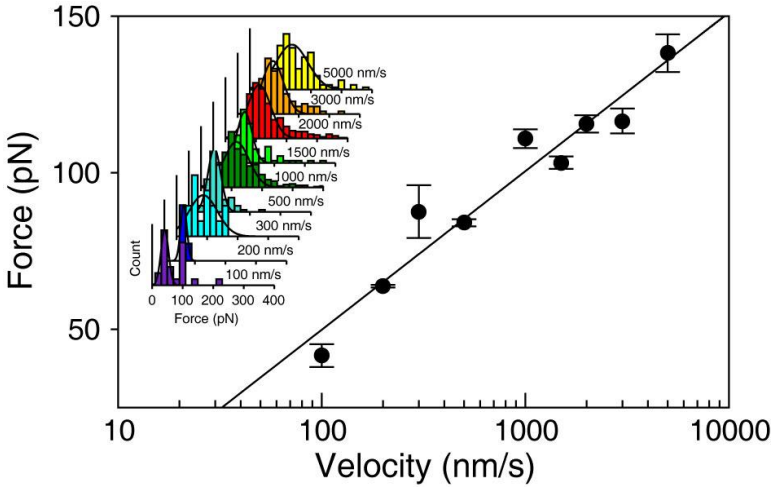

Fig. 3.1. At each velocity, the unfolding force peaks were sorted into 20 pN bins. Each binned histogram was fitted to a Gaussian curve to determine the position of the peak force. The error bars demonstrate the standard error.

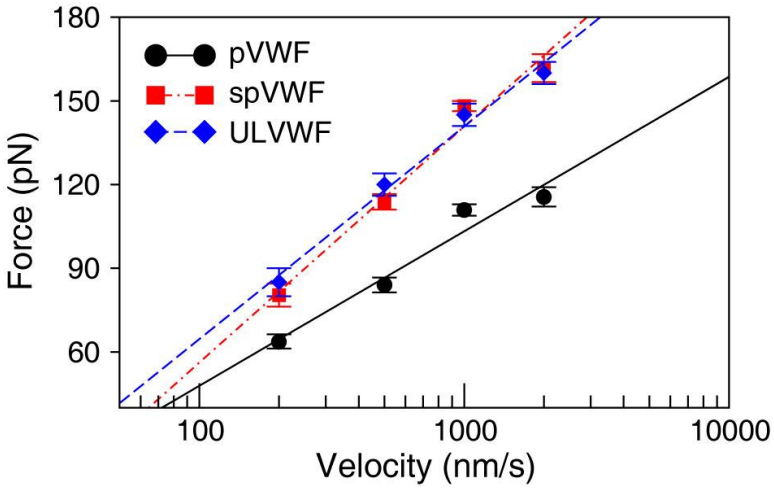

Fig. 3.2. Velocity-dependent peak unfolding forces of pVWF multimers, spVWF multimers, and ULVWF multimers. The peak unfolding forces increased logarithmically with pulling velocity. spVWF and ULVWF multimers have similar peak unfolding forces at all pulling velocities, and deviate from the peak unfolding force of pVWF multimers as the pulling velocities increase. The difference between peak unfolding forces diminishes at low pulling velocity.

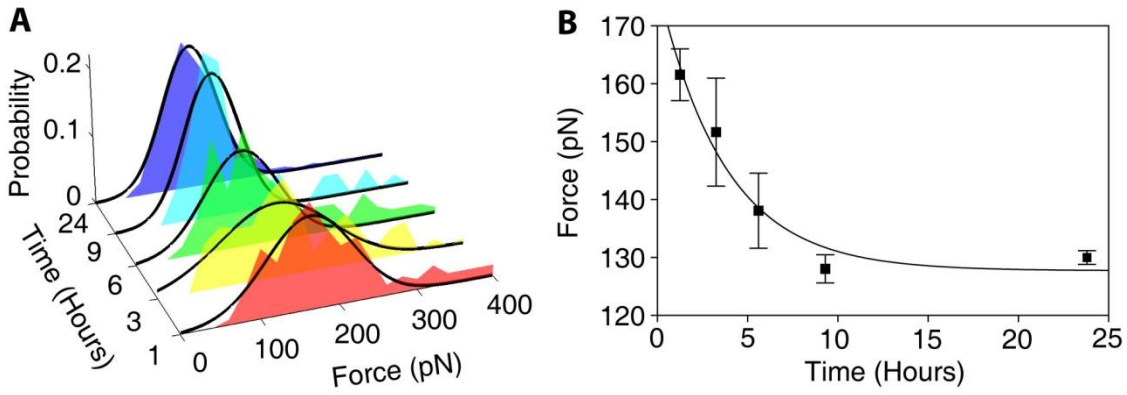

Fig. 3.3. Dynamics of spVWF. (A) Peak force distributions of spVWF as a function of time since exposure to a pathological high level of 100 dyn/cm^2 fluid shear. (B) The solid line shows the data fitted to a first order exponential decay.

3.2. Dynamics of VWF Multimers

To measure the kinetics in spVWF force experiments, peak unfolding force measurements of pVWF were conducted at different delay times after shear exposure. The spVWF unfolding force decreased over time, and reached its pre-shear-exposure force after 10 hours (Fig. 3.3A, B). Thus, the shear-induced change in pVWF to the spVWF multimeric conformation is reversible, but with a prolonged relaxation time of several hours. Fitting the data to the exponential equation $F(t) = F_P + (F_S - F_P)\exp(-t/\tau)$, where F_S is the peak force immediately after shear exposure, F_P is the equilibrium peak force, and τ is the time constant, yields F_S = 180 pN, F_P = 130 pN, and τ = 4 hours. The difference in the peak unfolding force between spVWF or ULVWF multimers and pVWF multimers is not significant at low pulling speed, indicating that the large multimeric VWF molecules had sufficient time to relax into a lower free energy, equilibrium state.

3.3. Evidence for VWF Conformation at the Domain Level

The force-extension curves (Fig. 2.1B, C) show that the unfolding force peaks correspond to the changes in the VWF multimeric conformation at the level of one or more domains within the VWF monomeric subunits. This conclusion is supported by i) the force-extension curves display a characteristic sawtooth pattern of repeated force peaks, resembling the known sequential unfolding of other multi-domain proteins [19]; ii) the increase in contour length after each peak, ΔL_c, is 30 nm, which is comparable to the contour length of an unfolded domain or an intermediate state; and iii) at 1000 nm/s pulling velocity, the value of the peak unfolding force was distributed at 100-150 pN, and varied linearly with the log of pulling velocity, as is typical of domain unfolding.

3.3.1. Change in Contour Length

The change in contour length associated with the unfolding force was determined by fitting the force-extension peaks to the WLC model of polymer elasticity [24]. Using the ΔL_c histogram of pVWF, and fitting the binned data to a double Gaussian distribution (Fig. 3.4), there was a major peak at 30(5) nm. This is a typical length for an unfolded domain of 90 amino acid residues. In addition, there was a minor peak at 60(5) nm, corresponding to an unfolded domain of 180 amino acid residues assuming 0.34 nm per residue [11, 28], consistent with domain unfolding.

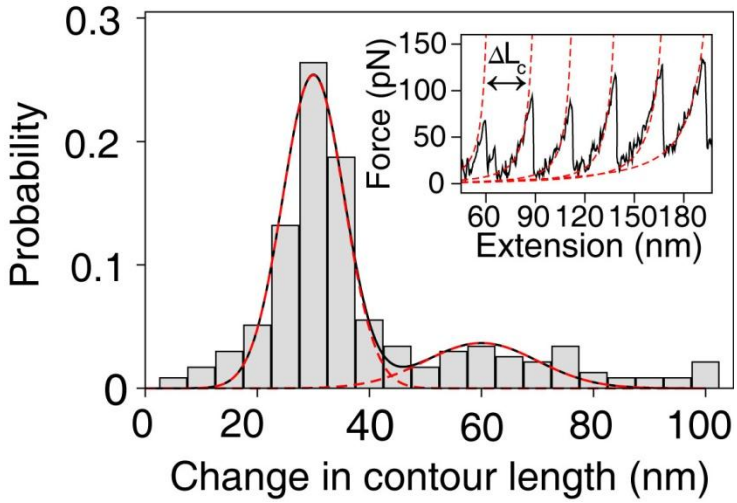

Fig. 3.4. Histogram of the change in contour length between unfolding peaks. The solid line (black) indicates a double Gaussian fit to the distribution, which has a major peak at 30 nm and a minor peak at 60 nm. Inset: The contour length of the peak unfolding forces was determined by fitting the force-extension curves to the WLC model (dashed red lines).

3.3.2. Number of Peak Unfolding Forces

In addition, by stretching VWF dimers under similar conditions, we found that there are up to 4 unfolding peaks per force-extension curve (Fig. 2.1C, Fig. 3.5), suggesting that there are up to two unfolding peaks per monomer. The two force peaks can be from the unfolding of two different domains or from two partial domains. This conclusion is illustrated when pulling eight serially linked titin I27 domain, $(I27)_8$, up to 8 unfolding peaks have been observed [19]. For comparison, pVWF curves have up to 10 force peaks, suggesting that there are up to 5 monomers at a given pull. The dimer force peak and change in contour length, ΔL_c, distributions are consistent with that of the multimer, further supporting the conclusion that the features in the multimeric VWF force-extension curves correspond to individual domain unfolding.

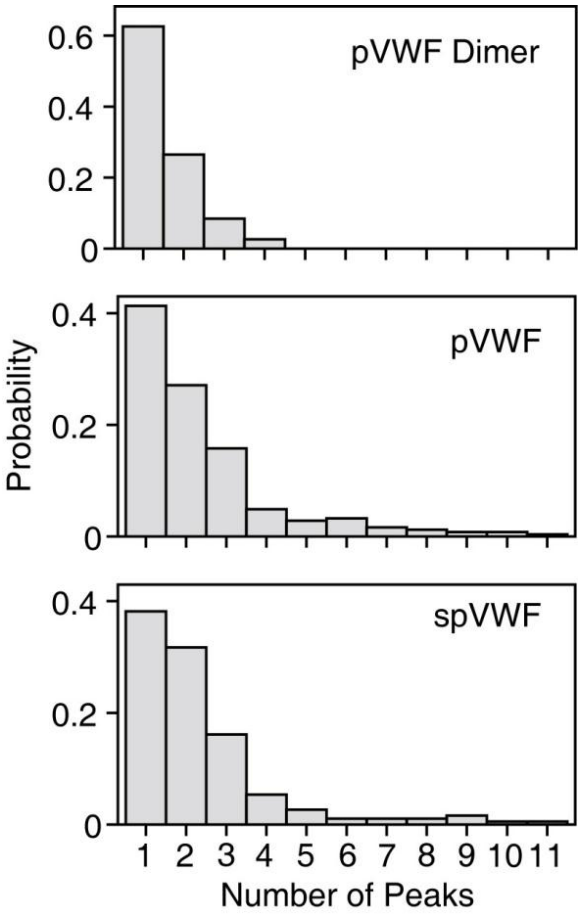

Fig. 3.5. Histograms of the number of peak unfolding forces for pVWF dimer, pVWF and spVWF multimer force-extension curves.

3.3.3. Contribution of A2 Domain to Force Signal

In the monomeric subunits of VWF multimers, the force peaks may be the combined result of unfolding different domains. It is likely, however, that there is a major contributor to the force signal. A probable candidate is the VWF A2 domain, because it does not have disulfide bonds, and has been observed to unfold in the pico-newton force range [29, 30]. The 177 residue A2 domain has a contour length of 64(4) nm, that is similar to our ΔL_c value of 60(5) nm, as well as to the value of 58(5) nm observed during unfolding of the A2 domain by optical tweezers [11]. The

most frequent ΔL_c observed, 30(5) nm, corresponds to the partial unfolding of about 40% of the residues in A2 [11, 29, 31]. The A1 and A3 domains contain disulfide bonds, which are unlikely to unfold during stretching experiments, because at a 100 nm/s pulling velocity, disulfide bonds typically rupture at 2 nN [32], a force much higher than the typical unfolding force (100-200 pN) observed in our study. Previous studies of the forced-unfolding of A1A2A3 triple domains also reveal that the VWF A2 domain can be partially or completely unfolded, possibly after inter-domain uncoupling [31, 33]. These findings suggest that the unfolding of a portion of the A2 domain in VWF monomeric subunits may be the main contributor to our unfolding force signals. Moreover, the altered A2 domain may deprotect the neighboring A1 domain, which permits the binding of A1 to platelet GPIbα receptors. We have ruled out that the change of unfolding force is simply due to more exposed A2 domains without intramolecular interactions, since such a configuration will only yield more unfolding peaks in a given pull (Fig. 3.5), but not a significantly altered unfolding force [17, 22].

3.4. Free Energy Landscape of Multimeric VWF

High shear stress (100 dyn/cm^2) was able to convert pVWF multimers to a conformation that was metastable, probably because of the lateral association of spVWF multimers, with a long relaxation time. Over several hours, the metastable state of spVWF crossed the energy barrier to return to its original pre-shear state. Using the time constant τ = 4 hours determined from the relaxation curve shown in

Fig. 3.3B, the activation free energy barrier from spVWF to pVWF, using the Arrhenius equation (see Eq. 2 in Chapter 2) is ΔG = 12-16 kcal/mol. The barrier height from an active state to an inactive state is comparable to protein unfolding, further supporting the explanation of domain conformational changes for the observed force peak change.

Fig. 3.6 highlights the free energy landscape [34] of different forms of VWF multimers. Our results suggest that pVWF multimers have different conformational states before and after shear exposure that unfold through different pathways (pathways 1 and 2). Proteins with multiple conformational states of different activities have been observed by force measurements [35]. pVWF multimers are in a native inactive state, but can be converted to a metastable active state (spVWF) by high shear stress. This state may be considered 'misfolded' since it is a non-native state [36]. The spVWF multimer's peak unfolding force, which is related to the barrier height [22, 37], is likely to be higher than that of pVWF multimers, because high shear stress induces the lateral association of several pVWF multimers into a fibrillar form spVWF multimers. Thus, shear effects on VWF monomeric A2 domains causes an associated increase in the exposure of platelet-binding VWF A1 domains.

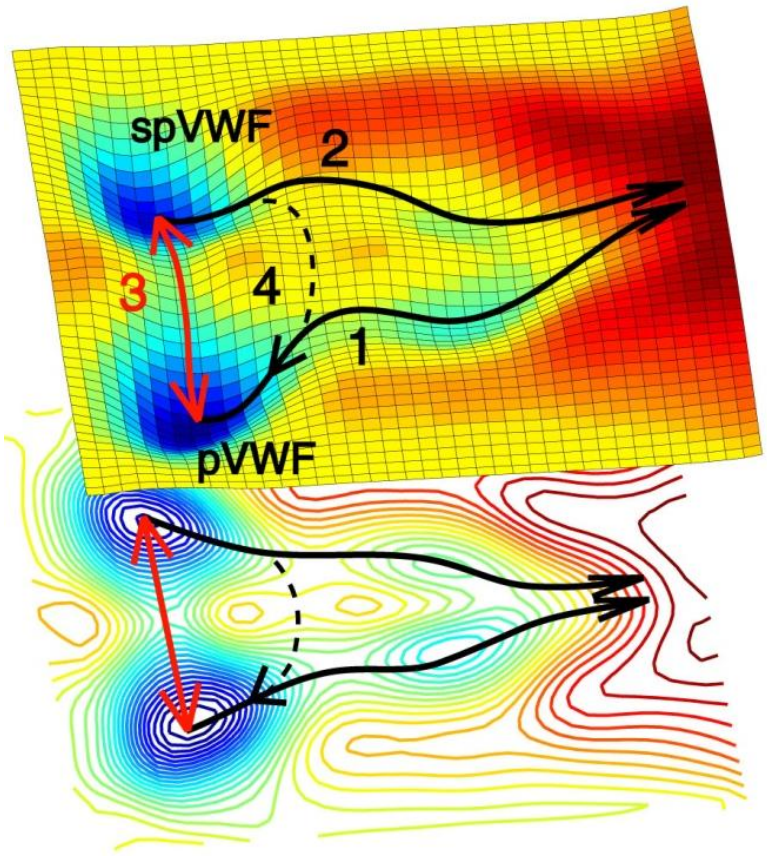

Fig. 3.6. Free energy landscape of multimeric VWF. pVWF is the native, equilibrium state. Fast stretching of pVWF molecules results in domain unfolding (pathway 1), while the spVWF domain unfolds through a different pathway (pathway 2), which has a higher unfolding free energy barrier, as reflected by the higher force peaks. High fluid shear stress switches pVWF to the spVWF state (pathway 3). At room temperature, the metastable spVWF state relaxes to the inactive pVWF state during a course of several hours (pathway 3). However, a small perturbation of the spVWF state, such as a small molecule or fluid drag, may lift the molecule out of its metastable state and cause it to fold back to its original state (pathway 4).

Chapter 4

Conclusion

In summary, our results demonstrate that pVWF multimers have different conformational states that unfold through different pathways before and after exposure to high shear stress. pVWF is in a native, inactive state that can be converted to a metastable active state, spVWF, by high shear stress. The peak unfolding force of spVWF multimers is higher than that of unsheared pVWF multimers, because high shear stress induces the lateral association of pVWF multimers into a fibrillar form. Thus, an increased intramolecular interaction shifts the domains to a different state that has a higher unfolding barrier. Shear-activated conformational changes in the A2 domains in VWF monomeric subunits of spVWF multimers may provoke an increased exposure of neighboring (platelet-binding) A1 domains. The effect is reversible over the course of several hours. It will be interesting to investigate if structural studies can resolve the two states and what

external factors, whether physical, chemical, or biological, may affect the stability of and switching rate between these states.

Chapter 5

Future Work

5.1. Investigating molecule-cell binding dynamics

At the site of a vessel injury, VWF can play a major role in the formation of platelet thrombi when in the form of ULVWF multimeric bodies [38-40]. During times without trauma and normal hemostasis, ULVWFs are cleaved by ADAMTS-13, preventing the smaller cleaved VWF particles from forming large platelet thrombi [10, 40-44]. We will observe the molecule-cell binding dynamics in real time to uncover the detailed mechanisms of molecule-cell interactions.

We will investigate the binding kinetics of VWF by varying the pulling velocity of the beads and using Bell's theory to obtain the rate of unbinding. We will stretch the molecules in the *x*-*y* direction, instead of *z*-axis, using receptors on beads to simulate platelet binding. In this geometry, the platelet binding will occur at a plane perpendicular to the view direction. We propose building on the method to

investigate the relative binding strength of the VWF and ULVWF multimers. We will determine the binding kinetics between ULVWF and GPIbα, their platelet receptor. We will determine if the binding is greater for ULVWF/GPIbα than pVWF/GPIbα. Experiments will also be conducted the addition of 1.0 mg/ml of ristocetin, which promotes binding between pVWF and its receptor. These results will resolve the question about whether the receptor-ligand binding is stronger for ULVWF than for pVWF. These findings will answer the question of whether the higher hemostatic activity in ULVWF is due to the more exposed binding sites or if there is a higher bond strength at the monomer level.

References

[1] J. Kim*, et al.*, "A mechanically stabilized receptor-ligand flex-bond important in the vasculature," *Nature,* vol. 466, pp. 992-995, 2010.

[2] Z. M. Ruggeri, "Von Willebrand factor," *Curr. Opin. Hematol.,* vol. 10, pp. 142-149, 2003.

[3] J. E. Sadler, "Biochemistry and genetics of von Willebrand factor," *Annu. Rev. Biochem.,* vol. 67, pp. 395-424, 1998.

[4] H. Choi*, et al.*, "Shear-induced disulfide bond formation regulates adhesion activity of von Willebrand factor," *J. Biol. Chem.,* vol. 282, pp. 35604-35611, 2007.

[5] J. L. Moake*, et al.*, "Unusually large plasma factor VIII: von Willebrand factor multimers in chronic relapsing thrombotic thrombocytopenic purpura," *New Engl. J. Med.,* vol. 307, pp. 1432-1435, 1982.

[6] W. E. Fowler*, et al.*, "Substructure of human von Willebrand factor," *J. Clin. Invest.,* vol. 76, pp. 1491-1500, 1985.

[7] K. Nishio*, et al.*, "Binding of platelet glycoprotein Ib alpha to von Willebrand factor domain A1 stimulates the cleavage of the adjacent domain A2 by ADAMTS13," *Proc. Natl Acad. Sci. USA,* vol. 101, pp. 10578-10583, 2004.

[8] J. E. Sadler, "Biomedicine: Contact - How platelets touch von Willebrand factor," *Science,* vol. 297, pp. 1128-1129, 2002.

[9] Q. Zhang*, et al.*, "Structural specializations of A2, a force-sensing domain in the ultralarge vascular protein von Willebrand factor," *Proc. Natl Acad. Sci. USA,* vol. 106, pp. 9226-9231, 2009.

[10] Z. Y. Tao*, et al.*, "Cleavage of ultralarge multimers of von Willebrand factor by C-terminal-truncated mutants of ADAMTS-13 under flow," *Blood,* vol. 106, pp. 141-143, 2005.

[11] X. Zhang*, et al.*, "Mechanoenzymatic cleavage of the ultralarge vascular protein von Willebrand factor," *Science,* vol. 324, pp. 1330-1334, 2009.

[12] J. F. Dong*, et al.*, "ADAMTS-13 rapidly cleaves newly secreted ultralarge von Willebrand factor multimers on the endothelial surface under flowing conditions," *Blood,* vol. 100, pp. 4033-4039, Dec 1 2002.

[13] D. D. Wagner, "Cell biology of von Willebrand factor," *Annu. Rev. Cell. Bio.,* vol. 6, pp. 217-246, 1990.

[14] J. Moake, "Thrombotic Microangiopathies: Multimers, Metalloprotease, and Beyond," *Cts-Clinical and Translational Science,* vol. 2, pp. 366-373, Oct 2009.

[15] S. W. Schneider*, et al.*, "Shear-induced unfolding triggers adhesion of von Willebrand factor fibers " *Proc. Natl Acad. Sci. USA,* vol. 104, pp. 7899-7903, 2007.

[16] M. H. Kroll*, et al.*, "Platelets and shear stress," *Blood,* vol. 88, pp. 1525-1541, 1996.

[17] C. A. Siedlecki*, et al.*, "Shear-dependent changes in the three-dimensional structure of human von Willebrand factor," *Blood,* vol. 88, pp. 2939-2950, 1996.

[18] H. C. Yeh*, et al.*, "Disulfide bond reduction of von Willebrand factor by ADAMTS-13," *J. Thromb. Haemost.,* vol. 8, pp. 2778-2788, 2010.
[19] M. Rief*, et al.*, "Reversible unfolding of individual titin immunoglobulin domains by AFM," *Science.,* vol. 276, pp. 1109-1112, 1997.
[20] P. E. Marszalek*, et al.*, "Mechanical unfolding intermediates in titin modules," *Nature,* vol. 402, pp. 100-103, 1999.
[21] M. Carrion-Vazquez*, et al.*, "Mechanical and chemical unfolding of a single protein: A comparison," *Proc. Natl Acad. Sci. USA,* vol. 96, pp. 3694-3699, 1999.
[22] N. C. Harris*, et al.*, "Experimental free energy surface reconstruction from single-molecule force spectroscopy using Jarzynski's equality," *Phys. Rev. Lett.,* vol. 99, pp. 068101, 2007.
[23] N. C. Harris and C. H. Kiang, "Velocity convergence of free energy surfaces from single-molecule measurements using Jarzynski's equality," *Phys. Rev. E,* vol. 79, p. 041912, 2009.
[24] C. Bustamante*, et al.*, "Entropic Elasticity of Lambda-Phage DNA," *Science,* vol. 265, pp. 1599-1600, 1994.
[25] B. Onoa*, et al.*, "Identifying kinetic barriers to mechanical unfolding of the T-thermophila ribozyme," *Science,* vol. 299, pp. 1892-1895, 2003.
[26] O. B. Bakajin*, et al.*, "Electrohydrodynamic stretching of DNA in confined environments," *Phys. Rev.Lett.,* vol. 80, pp. 2737-2740, 1998.
[27] J. L. Moake*, et al.*, "Involvement of large plasma von Willebrand factor (vWF) multimers and unusually large vWF forms derived from endothelial cells in shear stress-induced platelet aggregation," *J. Clin. Invest.,* vol. 78, pp. 1456-1461, 1986.
[28] F. Oesterhelt*, et al.*, "Unfolding pathways of individual bacteriorhodopsins," *Science,* vol. 288, pp. 143-146, 2000.
[29] C. Baldauf*, et al.*, "Shear-induced unfolding activates von Willebrand factor A2 domain for proteolysis," *J. Thromb. Haemost.,* vol. 7, pp. 2096-2105, Dec 2009.
[30] A. J. Jakobi*, et al.*, "Calcium modulates force sensing by the von Willebrand factor A2 domain," *Nature Commun.,* vol. 2, 2011.
[31] T. Wu*, et al.*, "Force-induced cleavage of single VWF A1A2A3 tridomains by ADAMTS-13," *Blood,* vol. 115, pp. 370-378, 2010.
[32] M. Grandbois*, et al.*, "How strong is a covalent bond?," *Science,* vol. 283, pp. 1727-1730, 1999.
[33] J. Y. Ying*, et al.*, "Unfolding the A2 Domain of Von Willebrand Factor with the Optical Trap," *Biophys. J.,* vol. 98, pp. 1685-1693, 2010.
[34] J. N. Onuchic*, et al.*, "Theory of protein folding: The energy landscape perspective," *Ann. Rev. Phys. Chem.,* vol. 48, pp. 545-600, 1997.
[35] J. Gore*, et al.*, "Mechanochemical analysis of DNA gyrase using rotor bead tracking," *Nature,* vol. 439, pp. 100-104, 2006.
[36] A. Sali*, et al.*, "How Does a Protein Fold," *Nature,* vol. 369, pp. 248-251, 19 1994.
[37] G. J. L. Wuite*, et al.*, "Single-molecule studies of the effect of template tension on T7 DNA polymerase activity," *Nature,* vol. 404, pp. 103-106, 2000.

[38] Z. M. Ruggeri, "The role of von Willebrand factor in thrombus formation," *Thromb. Res.,* vol. 102, pp. 55-59, 2007.

[39] M. Arya*, et al.*, "Ultralarge multimers on von Willebrand factor form spontaneous high-strength bonds with platelet glycoprotein Ib-IX complex studies using optical tweezers.," *Blood.,* vol. 99, pp. 3971-3977, 2002.

[40] J. F. Dong*, et al.*, "ADAMTS-13 rapidly cleaves newly secreted ultralarge von Willebrand factor multimers on the endothelial surface under flowing conditions," *Blood.,* vol. 100, pp. 4033-4039, 2002.

[41] L. Liu*, et al.*, "Platelet-derived VWF-cleaving metalloprotease ADAMTS-13," *J. Thromb. Haemost.,* vol. 3, pp. 2536-2544, 2005.

[42] R. A. Kumar*, et al.*, "Enhanced platelet adhesion and aggregation by endothelial cell-derived unusually large multimers of von Willebrand factor," *Biorheology,* vol. 43, pp. 681-691, 2006.

[43] N. Turner*, et al.*, "Human endothelial cells synthesize and release ADAMTS-13," *J. Thromb. Haemost.,* vol. 4, pp. 1396-1404, 2006.

[44] N. Turner*, et al.*, "ADAMTS-13 cleaves long von Willebrand factor multimeric strings anchored to endothelial cells in the absence of flow, platelets or conformation-altering chemicals," *J. Thromb. Haemost.,* vol. 7, pp. 229-232, 2009.